Imaging and manipulating pituitary function in the awake mouse

Citation for published version:
Hoa, O, Lafont, C, Fontanaud, P, Guillou, A, Kemkem, Y, Kineman, RD, Luque, RM, Coll, TF, Le Tissier, P & Mollard, P 2019, 'Imaging and manipulating pituitary function in the awake mouse', *Endocrinology* , vol. 160, no. 10, pp. 2271–2281. https://doi.org/10.1210/en.2019-00297

Digital Object Identifier (DOI):
10.1210/en.2019-00297

Published In:
Endocrinology

Imaging and manipulating pituitary function in the awake mouse

Authors: Ombeline Hoa[1,#], Chrystel Lafont[1], Pierre Fontanaud[1], Anne Guillou[1], Yasmine Kemkem[1], Rhonda D. Kineman[2,3], Raul M. Luque[4,5,6], Tatiana Fiordelisio Coll[7], Paul Le Tissier[8], Patrice Mollard[1,*]

Affiliations:; [1]IGF, CNRS, INSERM, Univ. Montpellier, F-34094 Montpellier, France, [2]Research and Development Division, Jesse Brown Veterans Affairs Medical Center, University of Illinois at Chicago, Chicago, Illinois, USA, [3]Department of Medicine, Section of Endocrinology, Diabetes, and Metabolism, University of Illinois at Chicago, Chicago, Illinois, USA, [4]Maimonides Institute for Biomedical Research of Cordoba (IMIBIC), Reina Sofia University Hospital, Córdoba, Spain, [5]Department of Cell Biology, Physiology and Immunology, University of Córdoba, Córdoba, Spain, [6]CIBER Fisiopatología de la Obesidad y Nutrición (CIBERobn); Córdoba, Spain, [7]Laboratorio de Neuroendocrinología Comparada, Departamento de Ecología y Recursos Naturales, Biología, Facultad de Ciencias, Universidad Nacional Autónoma de México, Ciudad Universitaria, 04510 México, DF, México, [8]University of Edinburgh, Centre for Discovery Brain Sciences, Edinburgh, EH8 9XD, UK

#New address: Center for Interdisciplinary Research in Biology (CIRB), Collège de France, CNRS, INSERM, PSL Research University, Paris, France

*Correspondence to:

Patrice Mollard, Institut de Génomique Fonctionnelle, 141 rue de la Cardonille, F-34000 Montpellier, France, tel. : +33 4334359270, email : patrice.mollard@igf.cnrs.fr

Running title: Pituitary initiative

Key words: In vivo imaging, optogenetic tools, viral infection, endocrine manipulation, hormone rhythms

Extensive efforts have been made to explore how the activities of multiple brain cells combine to alter physiology through imaging and cell-specific manipulation in different animal models. However, the temporal regulation of peripheral organs by the neuroendocrine factors released by the brain is poorly understood. We have established a suite of adaptable methodologies to interrogate *in vivo* the relationship of hypothalamic regulation with the secretory output of the pituitary gland, which has complex functional networks of multiple cell types intermingled with the vasculature. These allow imaging and optogenetic manipulation of cell activities in the pituitary gland in awake mouse models, in which both neuronal regulatory activity and hormonal output are preserved. This methodology is now readily applicable for longitudinal studies of short-lived events (e.g. calcium signals controlling hormone exocytosis) and slowly-evolving processes such as tissue remodelling in health and disease over a period of days to weeks.

Introduction

In the past decade, there has been an exponential increase in the technical development of novel tools allowing interrogation of the functional interactions of the complex architecture of the mammalian brain in health and disease. These have principally been developed in mouse models, where both organisation and function of the brain largely recapitulates that of higher mammals including humans (1). The availability of a wide-range of genetically-modified mice, combined with novel virus-based approaches to infect specific mouse brain regions, has allowed identification of specific cell-types, manipulation of neuronal circuits with optogenetic techniques and *in vivo* monitoring of cell activity. Combining these with recently developed optical techniques, such as the use of a gradient-index (GRIN) lens for imaging deep brain regions (2), has resulted in rapid mapping of the activity and connectivity of neuronal networks (3). Although the mammalian brain is exceptionally complex, the increasing prevalence of neurological and neuropsychiatric defects has recently inspired large-scale research programmes, such as the NIH Brain Research through Advancing Innovative Neuro-technologies (BRAIN) Initiative (4, 5), to meet this challenge.

The brain does not simply work as an isolated unit but forms a functional continuum with other physiological processes (6), especially with the endocrine systems that control basic body functions (7, 8). These endocrine systems share complex functional features with the brain, such as hierarchal multi-cellular organization (e.g. presence of "hub" cells which control neighbours (9, 10)), adaptive plasticity (11) and long-term memory (9), suggesting that studies of their function would benefit from application of the novel tools and techniques developed for neuroscience. This is exemplified by the pituitary gland, which acts as an intermediate between the brain and periphery, with endocrine and neural lobes (nerve terminals emanating from hypothalamic vasopressin and oxytocin neurons) connected to the brain by the pituitary stalk and surrounded by brain meninges (see Fig. 1). Interest in monitoring the *in vivo* function of this gland has recently been increased by large-scale *ex vivo* imaging, which has revealed 3D cell networks that are structurally and functionally organised within the endocrine anterior pituitary (also called the pars distalis); this cell network connectivity is essential for normal gland development (12), coordination of gene expression (13) and pulsatile release of

hormones to the periphery (8). To date, *in vivo* studies have been limited by the location of the pituitary on the ventral side of the brain, with extensive microsurgery required to expose the gland through the palate bone in terminally-anaesthetised mice to record and manipulate cell function (14). These surgical procedures preclude both longitudinal studies and functional investigation in awake mice.

Here, we describe a toolkit for imaging and manipulating pituitary cells *in vivo* over periods of days to weeks in awake mouse models. We have used these tools to: image the dynamics of pituitary microvascular function and cell signalling (calcium events); locally express exogenous proteins through injection of viral constructs within the parenchyma; and, optogenetically manipulate specific cell networks while monitoring their secretory outputs into the bloodstream. This range of techniques allows analysis of the pituitary gland in awake mammalian models in unparalleled detail, complementing large-scale studies of the brain to further understand neural control of complex physiological systems via endocrine signals.

Materials and Methods

Animals

Tg(Gh1-cre)bKnmn (called GH-Cre) (R Kineman, Jesse Brown Veterans Administration Medical Center, Chicago, USA) (15), ROSA26-*fl/fl*-ChR2-dtTomato and wild-type C57BL/6 mice (6–12 wk old) as indicated in figure legends, were housed in a 12-h light/12-h dark cycle (lights on at 0800 hours and off at 2000 hours) with food and water available *ad libitum*. All animal procedures were approved by the local ethical committee under agreement CEEA-LR-12185 according to EU Directive 2010/63/EU. Since this study included only one experimental group of animals, no randomization or blinding were required.

Stereotaxic injections of AAV

Adult GH-Cre mice and wild-type C57BL/6 were anesthetized with Ketamine/Xylazine (0.1/0.02 mg/g), placed in a stereotaxic apparatus, and given bilateral 1µL injections of AAV5-CAG-dflox-

GCaMP6s-WPRE-SV40 (2.52 × 10^13 GC/mL; Penn Vector Core), AAV5-CAG-GCaMP6s-WPRE-SV40 (2.23 × 10^13 GC/mL; Penn Vector Core), AAV2-CAG-GFP (gift from Margarita Arango, IGF, Montpellier), rAAV5/sspEMBOL-CBA-GFP (8 x 10^12 GC/mL; UNC Vector Core), rAAV8/sspEMBOL-CAG-GFP (8 x 10^12 GC/mL; UNC Vector Core) or rAAV9/sspEMBOL-CAG-GFP (9.2 x 10^12 GC/mL; UNC Vector Core) into the pituitary gland at a rate of 100 nL/min. Coordinates were -2.5mm antero-posterior, ±0.4mm lateral to midline, pointed as zero at the superior sagittal sinus. Two dorso-ventral positions were used for injection, 50µm and 400µm over the sella turca -6.15/5.75 mm for ventral injection and -5.6/5.3 mm for dorsal injection. Experiments were conducted from 4 weeks on after injection.

Optical imaging through a GRIN lens in awake head-fixed mice

Adult mice were anesthetized with Ketamine/Xylazine (0.1/0.02 mg/g) and placed in a stereotaxic apparatus to implant a GRIN lens (0.6 mm diameter, 1.5 pitch, 7.5mm length and 150µm working distance, GRINTECH Germany) immediately above the pituitary gland. After a large part of skull was exposed, the GRIN lens was placed in 20G1/2 Gauge needle (Ultra-Thin wall, Terumo, USA), with movement restricted by placing a metal rod above it. The needle was inserted at the coordinates -2.5mm antero-posterior, ±0.4mm lateral to midline pointed as zero at the superior sagittal sinus
-5.5/5.1 mm dorso-ventral. Then, the needle was removed with the metal rod kept in place so that the GRIN lens stayed in place at the dorsal side of the pituitary. Finally, the metal rod was removed. The GRIN lens and a head-plate were fixed with UV-retractable cement. Prior to and starting from two weeks after surgery, mice were habituated to the wheel and the head-plate fixation system under the microscope every two to three days. Four weeks after surgery, mice were placed on the wheel, the head-plate fixed, and fluorescence imaging was performed using a stereomicroscope (Zeiss Discovery V.12, Germany), which was fitted with a fluorescence lamp (Lambda LS, Sutter Instrument company, USA), a shutter (Lambda 10-B Smart Shutter, Sutter Instrument Company) and a CMOS ORCA Flash 4.0 camera (C11440 Hamamatsu, Japan), all controlled with MetaMorph 7.8.9 software (Molecular Devices, USA).

***In vivo* imaging in terminally-anesthetized mice**

Details of the methods can be found in Lafont et al. (2010) (14). In brief, male, 2- to 4-month-old transgenic GH-Cre mice and GH-ROSA26-*fl/fl*-ChR2-dtTomato mice on a C57Bl6 background were anesthetized by inhalation of isoflurane (1.5% in O2). After dividing the mandibular symphysis, the mucosa overlying the hard palate was parted by blunt dissection under a stereomicroscope to expose an area of palatal periosteal bone. This was thinned with a felt polisher (drill; World Precision Instruments, USA) and then removed with a hook and forceps. The exposed surface of the pituitary gland, visible through the hole in the bone, was continuously superfused with a physiological solution.

***In vivo* monitoring of blood flow and calcium signals**

Mice underwent surgery (see above) to visualize either the ventral (terminally-anesthetized animals) or the dorsal side (awake animals) of the pituitary gland. Using the ventral approach 100µl of tetramethylrhodamine isocyonate 150kDa dextran (Sigma Aldrich, USA) was injected into the jugular vein or in the retro-orbital sinus for GRIN lens approach. Imaging of blood flow was performed at 150 to 200 frames/sec using 545nm excitation and 570nm emission filters. When calcium signals were recorded *in vivo*, experiments were performed as described as above four weeks after stereotaxic injection of GCAMP6s-expressing AAV5. Multi-cellular calcium imaging was typically performed at 2-4 frames/sec, using 480nm excitation and 520nm emission filters.

Optogenetic photostimulation in awake mice

GH Cre x ROSA26-fl/fl-ChR2-dtTomato mice were anesthetized with Ketamine/Xylazine (0.1/0.02 mg/g) and placed in a stereotaxic apparatus to implant an optical fiber (diameter: 200µm, Doric Lenses, Canada) immediately above the pituitary gland (stereotaxic coordinates described above). The optical fiber was fixed using UV-retractable cement. Two weeks later, an optical fiber was connected to the one previously implanted, and laser stimulation (488nm) was delivered at 10mW and using

various patterns (frequency: 1Hz, exposure time: 300ms) while blood samples were collected as described below.

GH pulse profiling in mice and GH ELISA

A tail-tip blood collection procedure was used to sample blood from C57BL/6 adult mice or transgenic GH-Cre mice; 3µl blood samples were analyzed for GH content by ELISA (16).

iDISCO+

Pituitary glands were removed and fixed by overnight immersion in 4% paraformaldehyde. For the immunoflurescence labelling and clearing, an iDISCO+ clearing protocol was used as described in detail elsewhere(17). Primary antibodies were rat anti-Meca32 (1:100, BD Biosciences Cat# 550563, RRID:AB_393754)(18), guinea pig anti-GH (1:2500, NIDDK-NHPP Cat# AFP12121390, RRID:AB_2756840)(19), rabbit anti-GFP (1:250, Molecular Probes Cat# A-6455, RRID:AB_221570)(20) and secondary antibodies were anti-rat Alexa 647 (Jackson ImmunoResearch Labs Cat# 712-606-150, RRID:AB_2340695)(21), anti-guinea pig Alexa 510 (Jackson ImmunoResearch Labs Cat# 706-166-148, RRID:AB_2340461)(22) and anti-rabbit Alexa 488 (Molecular Probes Cat# A-21206, RRID:AB_141708)(23) (dilution: 1:2000). After clearing, transparent pituitary glands were mounted in well glass slides (065230, Dominique Dutscher) in DiBenzyl Ether (Sigma Aldrich). Coverslips were sealed with nail varnish.

Immunofluorescence staining in fixed pituitary slices

Pituitary glands were collected from terminally-anesthetized mice and fixed by overnight immersion in 4% paraformaldehyde at 4°C, serial cuts were done at 40µm-thick tissue sections using a vibratome (Leica, Germany). Combinations of the following antibodies were used: guinea pig anti- GH (NIDDK-NHPP Cat# AFP12121390, RRID:AB_2756840)(19), LH (NIDDK-NHPP Cat# rLHb, also AFP571292393, RRID:AB_2665511)(24), PRL (NIDDK-NHPP Cat# AFP65191, RRID:AB_2756841)(25), TSH (NIDDK-NHPP Cat# AFP9370793, RRID:AB_2756856)(26) or

ACTH (NIDDK-NHPP Cat# AFP71111591, RRID:AB_2756855)(27) (dilution: 1:2500), rabbit anti-GFP (1:250, Molecular Probes Cat# A-6455, RRID:AB_221570)(20) and rabbit anti-RFP (1:500, Rockland Cat# 600-401-379, RRID:AB_2209751)(28). Primary antibody incubation was performed in PBS, 0.1% Triton X-100, 2% BSA at 4 °C for 48 h. Sections were then incubated with secondary antibodies for 2h at room temperature. Secondary antibodies were anti-rabbit Alexa 488 (Molecular Probes Cat# A-21206, RRID:AB_141708)(23), anti-guinea pig Alexa 510 (Jackson ImmunoResearch Labs Cat# 706-166-148, RRID:AB_2340461)(22), Anti-Rat Alexa 647 (Jackson ImmunoResearch Labs Cat# 712-606-150, RRID:AB_2340695)(21), Anti-Guinea Pig Alexa 488 (Jackson ImmunoResearch Labs Cat# 706-545-148, RRID:AB_2340472)(29) and anti-rabbit 510 (Jackson ImmunoResearch Labs Cat# 711-166-152, RRID:AB_2313568)(30) (1:2000 in PBS, 0.1% Triton X-100, 2%BSA).

Confocal imaging

Fluorescence images of both sliced pituitaries and whole clarified pituitaries were acquired on a Zeiss LSM 780 confocal microscope with 20x, 40x, 63x objectives. Images were analyzed using Imaris (Bitplane, UK).

MRI image acquisition from mouse brain

Animals were scanned on a 9.4T Agilent Varian MRI scanner. A volumic RF43 antenna (Rapid Biomedical) was used. For image acquisition, mice were anesthetized with isoflurane and their heads secured with bite and ear bars. Respiration rate and heart rate were monitored. Animals were scanned using a spin echo sequence with the following parameters: Repetition time 500ms, echo time 10ms, 1 echo, averaging 16 times, matrix of 256 × 256 pixels in a FOV of 30x30mm, slices thickness 0.5mm. Total imaging time was 34 min.

Analysis

Blood flow changes were estimated from red blood cell velocities as previously described (14) and analysed using a two-tailed variance ratio test followed by a Mann–Whitney U test for any differences directly attributable to treatment application. Estimation of decay time (τ = 5sec) from calcium signals (27 single calcium transients) recorded in vivo was used to generate simulated calcium rises due to trains of calcium spikes firing at frequencies of either 0.4 or 1Hz. Spike frequencies high enough (1Hz) to generate robust plateau rises in cytosolic calcium (Figure supplement 6)(31) then guided selection of appropriate frequencies of laser light pulses during optogenetic experiments.

Results

Longitudinal optical monitoring of pituitary blood flow in awake mice

Unravelling the intricacies of pituitary function with cellular *in vivo* imaging studies lasting days to weeks requires optical access to the gland whilst maintaining both its integrity and that of surrounding tissue. The location of the pituitary (Fig. 1A-C, sagittal and coronal MRI sections of mouse heads and relative schemas, respectively), suggested that the least invasive strategy would be insertion of a GRIN lens though the cortex towards the dorsal side of the pituitary using a stereotaxic frame in anesthetized animals. To overcome the major challenge of crossing the meninges covering the ventral brain without damaging the nearby pituitary tissue (Fig. 1B), the GRIN lens was inserted into the lumen of a needle which was then retracted once the GRIN lens was located correctly (Fig. 1D). The GRIN lens was then fixed to the cranium with UV-retractable cement and a titanium bar with a central opening for the lens was attached to the skull. After at least 3-4 weeks of mouse habituation to being head-fixed under a stereomicroscope fitted with a x20 objective, with the body and limbs being able to move on a treadmill (Fig. 1E), pituitary blood flow was imaged for 0.5 to 2 hours in animals pre-injected in the retro-orbital sinus with fluorescent 150kDa dextran (Fig. 1F, video 1)(31). These *in vivo* imaging sessions were repeatable every 3-4 days and up to several months after GRIN lens implantation with no alteration in blood flow, assessed by measurements of red blood cell velocities (Fig. 1G). Imaging pituitary blood flow in awake mice using a GRIN lens with a numerical aperture of 0.5 provided image resolution similar to that obtained in terminally-anesthetized animals with ventral

surgery and imaged with a long-range (2 cm working distance, N.A. 0.5) objective (Fig. 1H, I) (14). All imaging sessions were performed between one and six months after GRIN lens implantation without noticeable changes of pituitary function, based on preservation of endogenous hormone rhythms (Figure supplement 1)(31). Thus implantation of thin GRIN lenses through two layers of meninges, one at the level of the cortex and the other covering the ventral side of the brain, allowed long-lasting *in vivo* imaging of the dorsal side of the pituitary whilst preserving characteristic features of pituitary function.

Selective viral delivery and fluorescent protein expression in the pituitary parenchyma

Local stereotaxic delivery for expression of specific genes, for example by viral transduction (2), has been an important tool for monitoring the activities of cells in selective brain regions. Whilst this approach has been applied to very large pituitary tumors by trans-auricular injection (32, 33), it has not been described in the pituitary of healthy mice. We developed stereotaxic delivery of viral particles that could easily be combined with *in vivo* imaging using GRIN lenses with minimal pituitary damage. We first inserted vertically the AAV-containing needle via the cortex and then positioned the needle tip to touch the palate bone. After waiting 5 min, the needle was retracted by 50µm and 400µm to target the ventral and dorsal regions of the pituitary, respectively (Fig. 2A). AAV particles were then injected using a controlled pneumatic pump to transduce cells with an expression cassette encoding the calcium sensor GCAMP6s (34) or GFP under the control of the strong ubiquitous CAG promoter. Virus was routinely injected in both pituitary "wings" (lateral regions are 500-700 µm thick). Pituitaries were then dissected and fixed 1, 14 and 28 days after viral injection (Fig. 2B-C). Although a small region of tissue damage was apparent one day after AAV injection using a needle with an outer diameter of 210µm diameter, this was markedly reduced or absent 2 weeks post-injection and apparently fully repaired after 4 weeks. Pituitary tissues were immunostained for fenestrated vessel markers (MECA32), pituitary hormones (e.g. GH) and GCAMP6s in thick pituitary sections (Fig. 2B, top left panels and tissue clarified with the iDISCO+ protocol (Fig. 2C, top right panel) (17). This showed that expression of AAV-CAG-expressed GCAMP6s could be detected 2 weeks post-infection (Fig. 2B-C, middle panels) but was increased and more extensive after 4 weeks

(Fig. 2B-C, bottom panels). Consistent with the apparently complete tissue recovery one month after AAV infection (Fig. 2B-C), endogenous (Fig. 2D) and hormonal responses to hypothalamic agonists (Figure supplement 2)(31) were unaltered following stereotaxic injection of AAV.

As the pituitary gland contains five endocrine cell types secreting specific hormones (PRL, LH/FSH, GH, ACTH and TSH), we tested the efficiency of viral transduction in each of these by a range of AAV serotypes expressing CAG promoter driven GFP. All pituitary hormonal cell types were transduced with variable efficiency depending of AAV serotype (Fig. 3, Figures supplement 3-5)(31). For all AAV serotypes, expression of GFP could readily be detected by immunostaining from constructs utilizing a CAG promoter but not those with a CMV promoter (data not shown).

Pituitary calcium signals in awake mice

Having successfully transduced pituitary cells with constructs expressing GCAMP6s by stereotaxic injection of AAV5-CAG-GCAMP6s, we then explored whether this could be used to monitor multicellular calcium signals in awake mice following AAV injection. GRIN lenses were implanted above the dorsal pituitary at the site where AAVs had previously been injected stereotaxically. One month after GRIN lens implantation, it was possible to monitor a wide range of profiles of pituitary calcium transients in awake mice (Fig. 4A-G, video 2)(31), with evidence of cell-cell coordination (Fig. 4B-4E, video 3)(31) similar to that previously reported in *ex vivo* studies on pituitary slice preparations (9, 11, 35). Of note, similar calcium activity was detected *in vivo* using a ventral imaging approach in anaesthetized mice (14) which had been injected with AAV5-CAG-GCAMP6s (Fig. 4H-I), suggesting that the GRIN lens implantation does not affect calcium signaling.

Optogenetic manipulation of pituitary hormone pulsatility in awake mice

The ability to implant lenses and optical devices into the pituitary of awake mice also enables control of the secretory activity of pituitary cells. For this, we used a Cre-lox strategy by crossing GH-Cre and

R26-*fl*-*fl*-ChR2-dtTomato mice, resulting in expression of ChR2 specifically in somatotrophs (GH-ChR2; Fig. 5A). To determine which blue laser illumination pattern was efficient at triggering hormone output from somatotrophs, we used the ventral imaging approach in anesthetized mice to stimulate the pituitary cells with a 400 µm diameter fiber optic positioned close to the pituitary surface (Fig. 5B) and measured GH in blood samples collected from the tail (Fig. 5C). The requirement for a 1Hz stimulation for 300ms to elicit a robust output of GH agrees with simulations of the generation of sustained trains of calcium spikes based on from *in vivo* calcium spike kinetics (Figure supplement 6)(31). Application of this pattern of laser light triggered GH pulses in awake GH-ChR2 mice chronically-implanted with an optical fiber which was located above the dorsal side of the pituitary (Fig. 5 D-E).

Discussion

By adapting approaches using stereotaxic to access the ventral side of the brain, we have successfully applied a wide range of tools and techniques for imaging and manipulating specific cell activities in the pituitary gland of awake mice. These technical developments now allow the study of the function of this gland and its intimate relationship with the brain in health and disease at a level hitherto not achievable in awake animal models. Analysis of dynamic pituitary function over periods of days to months in animals with intact interactions between multiple organs will provide important insight into a range of conditions with dysregulated physiological function which may occur at different level within an axis. For example, it is unclear to what extent altered pituitary, hypothalamic or ovarian function contributes to the dysregulated LH secretion which is a hallmark of the polycystic ovarian syndrome, the most common endocrine pathology in the reproductive age female (prevalence 7-15% of pre-menopausal women (36).

Live imaging with multi-cellular resolution in awake GRIN lens implanted mice is well suited to real-time studies of cell signals, as illustrated here with calcium signals that are essential for hormone exocytosis (8), and can be used to monitor cell-cell communication within the variety of intermingled

cell networks wiring the gland (12). As multi-cellular signal events can be directly combined with frequent blood microsamples and high-sensitive hormone ELISA (16), on-line monitoring of 'stimulus-secretion' coupling (37, 38) is now achievable at the organ (pituitary) level in awake animals, avoiding the well-described blunting of hypothalamic inputs by anesthetics (14). In addition, these studies will be augmented by combining laser light-control of cell functions with monitoring cell activity within the same field of view of the GRIN lens, which is now possible given the efficiency of optogenetic tools for the control of pituitary cell networks.

On-line monitoring and manipulation of *in vivo* stimulus-secretion coupling is now readily applicable to answer long-standing questions concerning pituitary gland integration of both brain and peripheral signals for the generation of pulsatile hormonal output. For example, it is now clear that dynamic pulses of corticotroph ACTH output is generated by both a combination of both hypothalamic (CRF and vasopressin) inputs and negative cortisol feedback (39). Future use of miniature imaging systems in GRIN lens-implanted animals (3) would allow monitoring and manipulation of corticotroph cell activity regulating the stress axis, with simultaneous modification of environmental conditions in freely-moving mouse models and study of behavioral effects. To date, such interrogation of the role of pituitary corticotrophs in the stress axis has been restricted to simpler animal models, such as larval zebrafish (40), which lack delivery of hypophysiotropic input via a portal blood system and thus may differ in important aspects to humans (8). An ability to manipulate pituitary cell output via optogenetic stimulation and/or inhibition will also allow dissection of the role of specific patterns of pituitary hormone output, for example the sexually dimorphic GH-dependent regulation liver gene expression (41). Male and female GH secretion patterns can now be optogenetically triggered irrespective of sex animal.

A remarkable feature of this suite of tools is their capacity to allow long-term pituitary imaging and manipulation in awake animals. With the restriction of studying adult animals, both short-lived cell events (as discussed above) and slowly-evolving remodelling of the tissue, such as angiogenesis and expansion/shrinkage of a cell population can now be examined over weeks to months in individual animals, which act as their own controls (42). This will notably be relevant for visualizing and

studying on-line potential repopulation of the pituitary with stem cells/progenitors (43-45) (e.g. fluorescent cells locally injected in immune-suppressed mice), which have the potential to restore cell populations in the hypoplastic pituitary. It will also be possible to explore the function of either sick or healthy tissue zones within one pituitary by local injection of, for example, tumor cells or a virus encoding CRISPR-driven gene mutation in Cas9-expressing mice (46, 47).

In summary, the ability to image at multiple time scales and manipulate the pituitary gland enables the interrogation of pituitary gland function in awake mammalian models and study of how it delivers highly-ordered hormone pulses essential for controlling body functions such as reproduction, growth, stress and metabolism. Since endocrine cells can be photo-painted *in situ* (10), longitudinal *in vivo* studies would give access to the history of cells (48) and how they interact with neighbours in their native environment (9, 49). Single-cell multiomics which include transcriptomics, epigenomics and proteomics (50) would then be applicable to individual pituitary cells which have been monitored for days to months in awake mouse models. Together with these newly-developed single-cell level techniques, application of our cellular *in vivo* imaging and manipulation toolkit to longitudinal studies of awake animal models will provide a unique ability to explore the origin and development of pituitary hormone defects.

Acknowledgements

We thank Margarita Arango (IGF, Montpellier, France) for helpful comments and suggestions about AAV experiments, Jerome Lecoq (Allen Inst., USA) for advices about the use of GRIN lenses, Danielle Carmignac (NIMR-MRC, London UK) for helpful suggestions about AAV injections, Yan Chastagnier (IGF, Montpellier, France) for help and advice about image analysis, and Muriel Asari for her schematic rendition of technical set-ups. Antibodies and Recombinant mouse Growth hormone and Prolactin were supplied by Dr. A.F. Parlow and NIDDK-National Hormone and Pituitary Program (NHPP, TORRANCE, CA). Authors were supported by grants from the Biotechnology and Biological Sciences Research Council, UK (BB/N007026/1) (P.L.T.), U.S. Department of Veterans Affairs,

Office of Research and Development Merit Award BX001114; and National Institutes of Health grant R01DK088133 (R.D.K), Junta de Andalucía (CTS-1406, BIO-0139), ISCIII-FIS (PI16/00264) (R.M.L.), ANR-CONACyT 273513, Estancia Sabática apoyada con el Programa PASPA-DGAPA UNAM (T.F.C) , the Agence Nationale de la Recherche (ANR 12 BSV1 0032-01, ANR-15-CE14-0012-01), France-Bioimaging (INBS10-GaL/AR-11/12), Institut National de la Santé et de la Recherche Médicale, Centre National de la Recherche Scientifique, Université de Montpellier, and Fondation pour la Recherche Médicale (DEQ20150331732) (P.M.). OH was supported by a PhD fellowship from Fondation pour la Recherche Médicale (FDT20160435494). We would also like to thank all members of the Montpellier core facilities IPAM and BioNanoNMRI for unconditional support and thoughtful comments during the course of this work.

References

1. Buzsaki G, Logothetis N, Singer W 2013 Scaling brain size, keeping timing: evolutionary preservation of brain rhythms. Neuron 80:751-764
2. Deisseroth K, Schnitzer MJ 2013 Engineering approaches to illuminating brain structure and dynamics. Neuron 80:568-577
3. Li Y, Mathis A, Grewe BF, Osterhout JA, Ahanonu B, Schnitzer MJ, Murthy VN, Dulac C 2017 Neuronal Representation of Social Information in the Medial Amygdala of Awake Behaving Mice. Cell 171:1176-1190 e1117
4. Ecker JR, Geschwind DH, Kriegstein AR, Ngai J, Osten P, Polioudakis D, Regev A, Sestan N, Wickersham IR, Zeng H 2017 The BRAIN Initiative Cell Census Consortium: Lessons Learned toward Generating a Comprehensive Brain Cell Atlas. Neuron 96:542-557
5. Jorgenson LA, Newsome WT, Anderson DJ, Bargmann CI, Brown EN, Deisseroth K, Donoghue JP, Hudson KL, Ling GS, MacLeish PR, Marder E, Normann RA, Sanes JR, Schnitzer MJ, Sejnowski TJ, Tank DW, Tsien RY, Ugurbil K, Wingfield JC 2015 The BRAIN Initiative: developing technology to catalyse neuroscience discovery. Philosophical transactions of the Royal Society of London Series B, Biological sciences 370
6. Sudhof TC 2017 Molecular Neuroscience in the 21st Century: A Personal Perspective. Neuron 96:536-541
7. Herbison AE 2016 Control of puberty onset and fertility by gonadotropin-releasing hormone neurons. Nature reviews Endocrinology 12:452-466
8. Le Tissier P, Campos P, Lafont C, Romano N, Hodson DJ, Mollard P 2017 An updated view of hypothalamic-vascular-pituitary unit function and plasticity. Nature reviews Endocrinology 13:257-267
9. Hodson DJ, Schaeffer M, Romano N, Fontanaud P, Lafont C, Birkenstock J, Molino F, Christian H, Lockey J, Carmignac D, Fernandez-Fuente M, Le Tissier P, Mollard P 2012 Existence of long-lasting experience-dependent plasticity in endocrine cell networks. Nature communications 3:605
10. Johnston NR, Mitchell RK, Haythorne E, Pessoa MP, Semplici F, Ferrer J, Piemonti L, Marchetti P, Bugliani M, Bosco D, Berishvili E, Duncanson P, Watkinson M, Broichhagen J, Trauner D, Rutter GA, Hodson DJ 2016 Beta Cell Hubs Dictate Pancreatic Islet Responses to Glucose. Cell Metab 24:389-401
11. Sanchez-Cardenas C, Fontanaud P, He Z, Lafont C, Meunier AC, Schaeffer M, Carmignac D, Molino F, Coutry N, Bonnefont X, Gouty-Colomer LA, Gavois E, Hodson DJ, Le Tissier P, Robinson IC, Mollard P 2010 Pituitary growth hormone network responses are sexually dimorphic and regulated by gonadal steroids in adulthood. Proceedings of the National Academy of Sciences of the United States of America 107:21878-21883
12. Budry L, Lafont C, El Yandouzi T, Chauvet N, Conejero G, Drouin J, Mollard P 2011 Related pituitary cell lineages develop into interdigitated 3D cell networks. Proceedings of the National Academy of Sciences of the United States of America 108:12515-12520
13. Featherstone K, Hey K, Momiji H, McNamara AV, Patist AL, Woodburn J, Spiller DG, Christian HC, McNeilly AS, Mullins JJ, Finkenstadt BF, Rand DA, White MR, Davis JR 2016 Spatially coordinated dynamic gene transcription in living pituitary tissue. Elife 5:e08494
14. Lafont C, Desarmenien MG, Cassou M, Molino F, Lecoq J, Hodson D, Lacampagne A, Mennessier G, El Yandouzi T, Carmignac D, Fontanaud P, Christian H, Coutry N, Fernandez-Fuente M, Charpak S, Le Tissier P, Robinson IC, Mollard P 2010 Cellular in vivo imaging reveals coordinated regulation of pituitary microcirculation and GH cell network function. Proceedings of the National Academy of Sciences of the United States of America 107:4465-4470

15. Luque RM, Amargo G, Ishii S, Lobe C, Franks R, Kiyokawa H, Kineman RD 2007 Reporter expression, induced by a growth hormone promoter-driven Cre recombinase (rGHp-Cre) transgene, questions the developmental relationship between somatotropes and lactotropes in the adult mouse pituitary gland. Endocrinology 148:1946-1953
16. Steyn FJ, Huang L, Ngo ST, Leong JW, Tan HY, Xie TY, Parlow AF, Veldhuis JD, Waters MJ, Chen C 2011 Development of a method for the determination of pulsatile growth hormone secretion in mice. Endocrinology 152:3165-3171
17. Renier N, Adams EL, Kirst C, Wu Z, Azevedo R, Kohl J, Autry AE, Kadiri L, Umadevi Venkataraju K, Zhou Y, Wang VX, Tang CY, Olsen O, Dulac C, Osten P, Tessier-Lavigne M 2016 Mapping of Brain Activity by Automated Volume Analysis of Immediate Early Genes. Cell 165:1789-1802
18. RRID:AB_393754, https://scicrunch.org/resolver/AB_393754
19. RRID:AB_2756840, https://scicrunch.org/resolver/AB_2756840
20. RRID:AB_221570, https://scicrunch.org/resolver/AB_221570
21. RRID:AB_2340695, https://scicrunch.org/resolver/AB_2340695
22. RRID:AB_2340461, https://scicrunch.org/resolver/AB_2340461
23. RRID:AB_141708, https://scicrunch.org/resolver/AB_141708
24. RRID:AB_2665511, https://scicrunch.org/resolver/AB_2665511
25. RRID:AB_2756841, https://scicrunch.org/resolver/AB_2756841
26. RRID:AB_2756856, https://scicrunch.org/resolver/AB_2756856
27. RRID:AB_2756855, https://scicrunch.org/resolver/AB_2756855
28. RRID:AB_2209751, https://scicrunch.org/resolver/AB_2209751
29. RRID:AB_2340472, https://scicrunch.org/resolver/AB_2340472
30. RRID:AB_2313568, https://scicrunch.org/resolver/AB_2313568
31. Materials to be uploaded to Dryad.
32. Riley DJ, Nikitin AY, Lee WH 1996 Adenovirus-mediated retinoblastoma gene therapy suppresses spontaneous pituitary melanotroph tumors in Rb+/- mice. Nat Med 2:1316-1321
33. Walls GV, Lemos MC, Javid M, Bazan-Peregrino M, Jeyabalan J, Reed AA, Harding B, Tyler DJ, Stuckey DJ, Piret S, Christie PT, Ansorge O, Clarke K, Seymour L, Thakker RV 2012 MEN1 gene replacement therapy reduces proliferation rates in a mouse model of pituitary adenomas. Cancer Res 72:5060-5068
34. Chen TW, Wardill TJ, Sun Y, Pulver SR, Renninger SL, Baohan A, Schreiter ER, Kerr RA, Orger MB, Jayaraman V, Looger LL, Svoboda K, Kim DS 2013 Ultrasensitive fluorescent proteins for imaging neuronal activity. Nature 499:295-300
35. Bonnefont X, Lacampagne A, Sanchez-Hormigo A, Fino E, Creff A, Mathieu MN, Smallwood S, Carmignac D, Fontanaud P, Travo P, Alonso G, Courtois-Coutry N, Pincus SM, Robinson IC, Mollard P 2005 Revealing the large-scale network organization of growth hormone-secreting cells. Proceedings of the National Academy of Sciences of the United States of America 102:16880-16885
36. Hayes MG, Urbanek M, Ehrmann DA, Armstrong LL, Lee JY, Sisk R, Karaderi T, Barber TM, McCarthy MI, Franks S, Lindgren CM, Welt CK, Diamanti-Kandarakis E, Panidis D, Goodarzi MO, Azziz R, Zhang Y, James RG, Olivier M, Kissebah AH, Reproductive Medicine N, Stener-Victorin E, Legro RS, Dunaif A 2015 Genome-wide association of polycystic ovary syndrome implicates alterations in gonadotropin secretion in European ancestry populations. Nature communications 6:7502
37. Neher E, Marty A 1982 Discrete changes of cell membrane capacitance observed under conditions of enhanced secretion in bovine adrenal chromaffin cells. Proceedings of the National Academy of Sciences of the United States of America 79:6712-6716
38. Thomas P, Surprenant A, Almers W 1990 Cytosolic Ca2+, exocytosis, and endocytosis in single melanotrophs of the rat pituitary. Neuron 5:723-733
39. Walker JJ, Spiga F, Waite E, Zhao Z, Kershaw Y, Terry JR, Lightman SL 2012 The origin of glucocorticoid hormone oscillations. PLoS biology 10:e1001341

40. De Marco RJ, Thiemann T, Groneberg AH, Herget U, Ryu S 2016 Optogenetically enhanced pituitary corticotroph cell activity post-stress onset causes rapid organizing effects on behaviour. Nature communications 7:12620
41. Waxman DJ, O'Connor C 2006 Growth hormone regulation of sex-dependent liver gene expression. Mol Endocrinol 20:2613-2629
42. Pilz GA, Bottes S, Betizeau M, Jorg DJ, Carta S, Simons BD, Helmchen F, Jessberger S 2018 Live imaging of neurogenesis in the adult mouse hippocampus. Science 359:658-662
43. Andoniadou CL, Matsushima D, Mousavy Gharavy SN, Signore M, Mackintosh AI, Schaeffer M, Gaston-Massuet C, Mollard P, Jacques TS, Le Tissier P, Dattani MT, Pevny LH, Martinez-Barbera JP 2013 Sox2(+) stem/progenitor cells in the adult mouse pituitary support organ homeostasis and have tumor-inducing potential. Cell Stem Cell 13:433-445
44. Perez Millan MI, Brinkmeier ML, Mortensen AH, Camper SA 2016 PROP1 triggers epithelial-mesenchymal transition-like process in pituitary stem cells. Elife 5
45. Rizzoti K, Akiyama H, Lovell-Badge R 2013 Mobilized adult pituitary stem cells contribute to endocrine regeneration in response to physiological demand. Cell Stem Cell 13:419-432
46. Swiech L, Heidenreich M, Banerjee A, Habib N, Li Y, Trombetta J, Sur M, Zhang F 2015 In vivo interrogation of gene function in the mammalian brain using CRISPR-Cas9. Nat Biotechnol 33:102-106
47. VanDusen NJ, Guo Y, Gu W, Pu WT 2017 CASAAV: A CRISPR-Based Platform for Rapid Dissection of Gene Function In Vivo. Curr Protoc Mol Biol 120:31 11 31-31 11 14
48. Singh SP, Janjuha S, Hartmann T, Kayisoglu O, Konantz J, Birke S, Murawala P, Alfar EA, Murata K, Eugster A, Tsuji N, Morrissey ER, Brand M, Ninov N 2017 Different developmental histories of beta-cells generate functional and proliferative heterogeneity during islet growth. Nature communications 8:664
49. van der Meulen T, Mawla AM, DiGruccio MR, Adams MW, Nies V, Dolleman S, Liu S, Ackermann AM, Caceres E, Hunter AE, Kaestner KH, Donaldson CJ, Huising MO 2017 Virgin Beta Cells Persist throughout Life at a Neogenic Niche within Pancreatic Islets. Cell Metab 25:911-926 e916
50. Macaulay IC, Ponting CP, Voet T 2017 Single-Cell Multiomics: Multiple Measurements from Single Cells. Trends Genet 33:155-168

Figure legends

Figure 1. In vivo imaging of pituitary blood flow in the awake mouse. (**A**) Sagittal MRI view of the mid-brain from a female mouse. Red rectangle indicates pituitary location below the ventral side of the brain. Scale bar, 3mm. (**B**) Drawing of a sagittal view of the hypothalamus-pituitary system. Ht, hypothalamus; tv, third ventrical; me, median eminence; ps, pituitary stalk; d, dura mater (in red); ar, arachnoid mater (in blue); pn, pars nervosa; pi, pars intermedia; pd, pars distalis; sb, sphenoidal bone. Scale bar, 300µm. (**C**) Coronal MRI view of the brain of a female mouse. Red rectangle indicates pituitary location. Scale bar, 3mm. (**D**) Schema showing the GRIN lens implantation in the arachnoid matter region above the dorsal side of the pituitary. Downward (1) and upward (2) arrows indicate the

sequential needle movements when the GRIN lens is positioned above the pituitary. Scale bar, 300µm. (**E**) Head-fixed in vivo imaging of an awake mouse implanted with a GRIN lens which provides an optical relay between the microscope and pituitary gland. (**F**) Head-fixed in vivo imaging of pituitary capillaries at low (left panel) and high magnification (right panel). Scale bar, 100µm; representative image of n = 5 female mice. (**G**) Example of longitudinal monitoring of red blood cell velocities in the same pituitary field viewed from one to six months after GRIN lens implantation; n = 21 to 43 vessels analyzed per animal, n= 4 female mice. (**H**) Schematic arrangement of the ventral in vivo imaging approach in terminally-anesthetized mice (14). (**I**) Ventral in vivo imaging of pituitary capillaries at the level of the pituitary parenchyma (left panel) and entrance (right panel) of different male mice. Scale bar, 100µm. See also Figure supplement 1(31).

Figure 2. AAV injection into the pituitary. (**A**) Following bi-lateral AAV injection in anesthetized mice, pituitaries were dissected from terminally anesthetized animals from 1 to 28 days after GCAMP6s-expressing AAV5 injection, fixed and subjected to immunostaining and imaging. (**B**) and (**C**) pituitary sections and whole gland (iDISCO+ protocol), respectively. Immunostaining for GH (cells pseudo-coloured in white), GCAMP6s (green) and MECA32 (a marker of fenestrated capillaries, magenta); representative images of n = 2-4 male mice per condition. White arrows indicate presumed needle tissue damage. Scale bars, 50µm (left panels) and 300µm (right panels), respectively. (**D**) Endogenous GH pulses prior to and one month after AAV5 injection in the same animal. 3µl blood samples were collected every 5 min at the tail-tip and GH content was then measured using a high-sensitive Elisa assay. See also Figure supplement 2(31).

Figure 3. Percentage of infected cells per pituitary cell type. (**A**) Infection efficiency by different AAV serotypes (2, 5, 8 and 9) of endocrine cell types (6 tissue sections/pituitary, n = 3 female mice). The percentage of infected cells was counted under microscopic observation within each field of infected cells. (**B**) Examples of co-labelling of endocrine pituitary cells infected by AAV5-CAG-GFP

particles (fixed pituitary sections followed by dual immunostaining against hormones and GFP). Scale bars, 20µm. See also Figures supplement 3-5(31).

Figure 4. *In vivo* calcium imaging in pituitary cells in the awake mouse. (**A**) Schematic arrangement of calcium imaging in head-fixed animals injected with AAV5-CAG-GCAMP6s particles into the pituitary. (**B**) Field of GCAMP6s cells viewed from the dorsal pituitary side with the selection of cells as ROIs shown in colored circles in A. Scale bar, 40µm; representative image of n=3 female mice. (**C**) Coordinated calcium spikes recorded in cells shown in B. (**D**) Calcium spikes recorded at 10 frames/sec in cells shown in B. (**E**) Mosaic of GCAMP6s images (bottom right, recording time in sec) show a coordinated increase in calcium spike firing. Scale bar, 50µm (**F**) and (**G**). Two examples of calcium recordings in other female animals injected with AAV5-CAG-GCAMP6s particles. Scale bar, 100µm. (**H**) and (**I**) Calcium signals in pituitary cells (I) imaged from the ventral side in a terminally-anesthetized animal (H); representative image and trace of n = 2 male mice.

Figure 5. Optogenetic stimulation of GH pulses *in vivo*. (**A**) Co-labelling of dtTomato and GH in the pituitary from a GH-Cre mouse injected with Cre-activated AAV5-GAG-ChR2-dtTomato particles. (**B**) Laser light illumination of the ventral pituitary side in terminally-anesthetized mice subjected to tail-tip blood sampling (3µl every 3 min). (**C**) In experimental conditions as in B, trains of blue laser light pulses (300 msec pulses at 1Hz) were able to trigger GH pulses (n = 5 male mice). (**D**) Laser light illumination of the pituitary in the awake mouse in which tail-tip blood sampling was carried out. (**E**) GH pulses triggered by a train of laser light pulses (300 msec pulses at 1Hz) in GH-Cre mice injected with Cre-selective AAV5-GAG-ChR2-dtTomato particles (n = 5 male mice). See also Figure supplement 6(31).

Supplementary information

Figure supplement 1. Endogenous GH pulses in 3 male mice implanted with a GRIN-lens. Related to Figure 1. In awake animals, 3µl blood aliquots were tail-tip collected every 10min.

Figure supplement 2. Prolactin secretion response in response to the D2 receptor antagonist domperidone (Dp) in mice. Related to Figure 2. In awake animals prior to (**A**) or one month after pituitary infection (**B**) with AAV5-CAG-GFP virus particles (about 80% of lactotrophs were infected), domperidone (20 mg/kg (Abcam Biochemicals) was injected i.p. and tail-tip blood samples were then processed using a high-sensitive mPRL Elisa; n = 4 female mice.

Figure supplement 3. Representative examples of co-labelling of endocrine pituitary cells infected by AAV2-CAG-GFP particles (fixed pituitary sections) in 3 tissue sections /pituitary of 3 female mice. Related to Figure 3. Scale bars, 20µm.

Figure supplement 4. Representative examples of co-labelling of endocrine pituitary cells infected by AAV8-CAG-GFP particles (fixed pituitary sections) in 3 tissue sections /pituitary of 3 female mice. Related to Figure 3. Scale bars, 20µm.

Figure supplement 5. Representative examples of co-labelling of endocrine pituitary cells infected by AAV9-CAG-GFP particles (fixed pituitary sections) in 3 tissue sections /pituitary of 3 female mice. Related to Figure 3. Scale bars, 20µm.

Figure supplement 6. Representation of simulated trains of *in vivo* calcium spikes from pituitary cells. Based on simulated calcium spikes with a 5sec decay time (see Materials and Methods for

details), stimulation at frequencies of 1Hz (A), but not 0.4 Hz (B) was efficient at eliciting a robust calcium plateau rise. Related to Figure 5.

Video 1. Head-fixed *in vivo* imaging of pituitary blood flow (see Figure 1F, right panel). 100 frames/sec.

Video 2. Head-fixed *in vivo* imaging of pituitary cells expressing GCAMP6s (see Figure 4G). 10 frames/sec.

Video 3. Head-fixed *in vivo* imaging of pituitary cells expressing GCAMP6s, which display coordinated calcium signals (see Figures 4B-4E). 10 frames/sec.

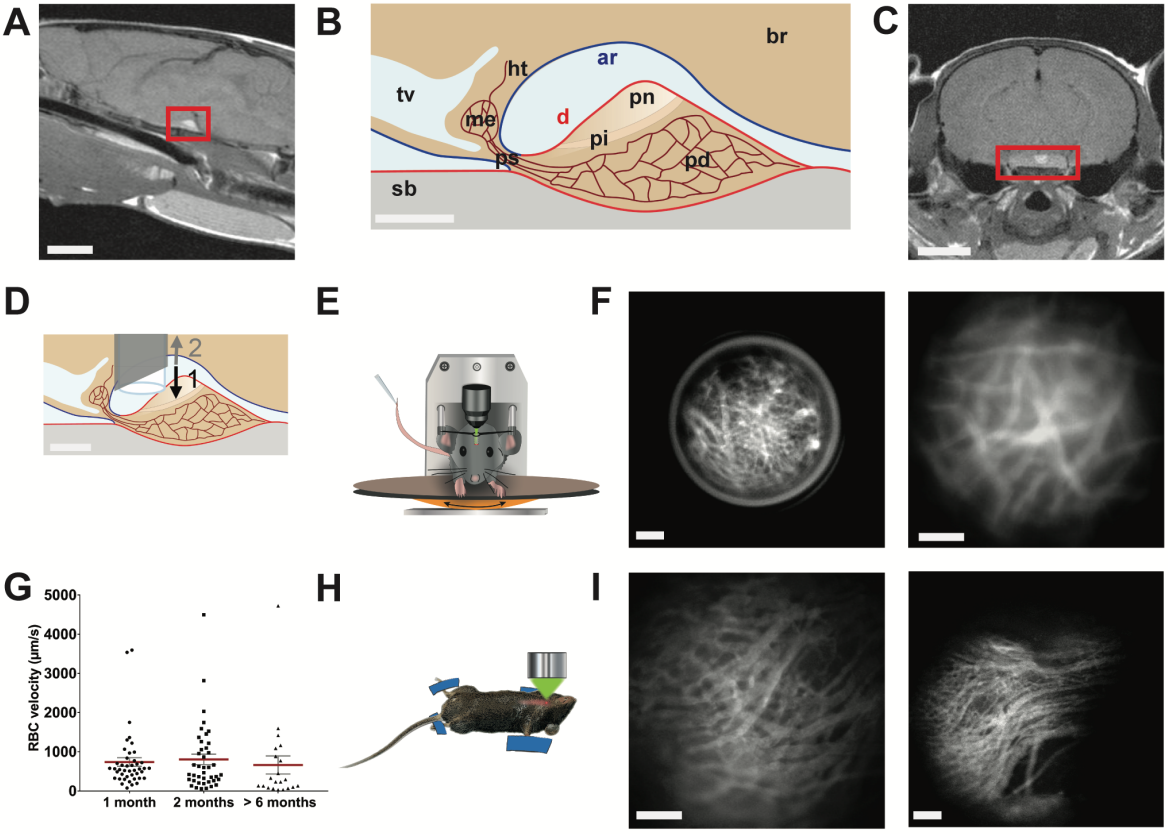
A
B
br
ar
ht
tv
pn
me
d
pi
ps
pd
sb
C
D
2
1
E
F
G
RBC velocity (µm/s)
5000
4000
3000
2000
1000
0
1 month
2 months
> 6 months
H
I

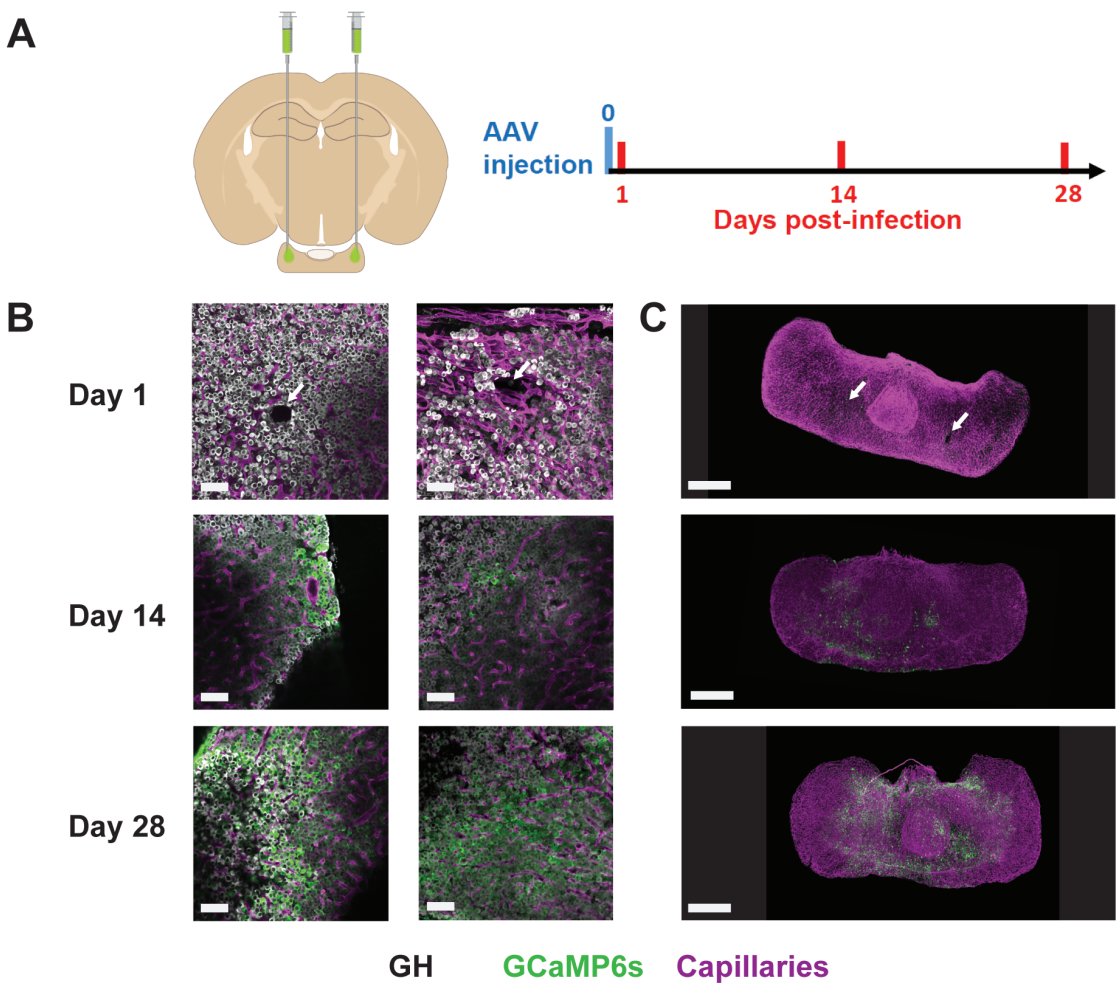
A
AAV injection
0
1
14
28
Days post-infection
B
Day 1
Day 14
Day 28
C
GH
GCaMP6s
Capillaries

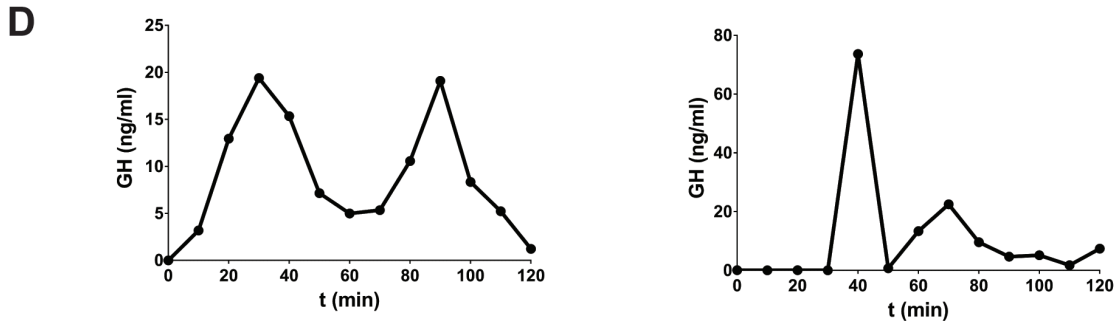
D
GH (ng/ml)
t (min)
GH (ng/ml)
t (min)

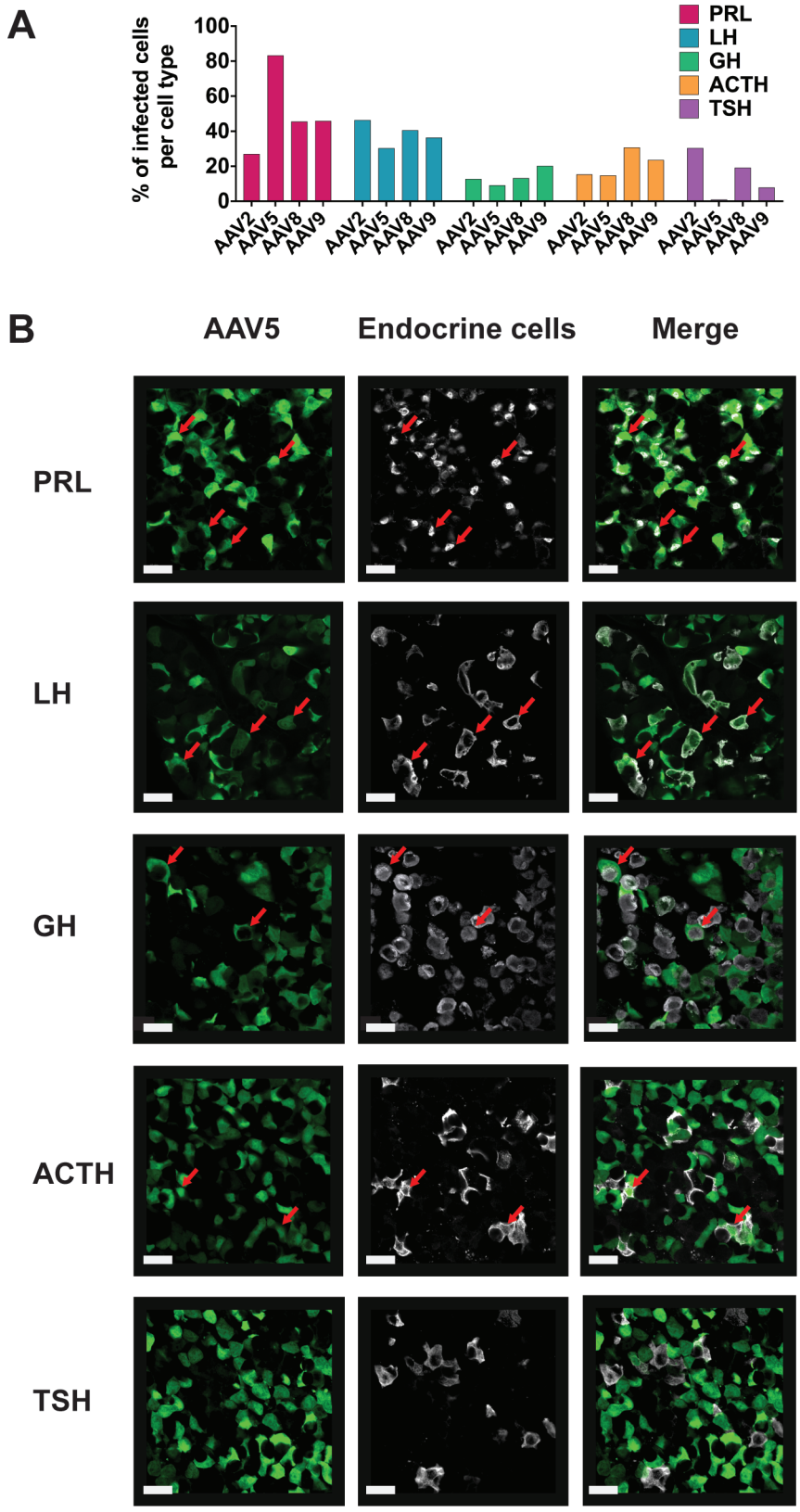
A
% of infected cells per cell type
100
80
60
40
20
0
PRL
LH
GH
ACTH
TSH
AAV2
AAV5
AAV8
AAV9
B
AAV5
Endocrine cells
Merge
PRL
LH
GH
ACTH
TSH

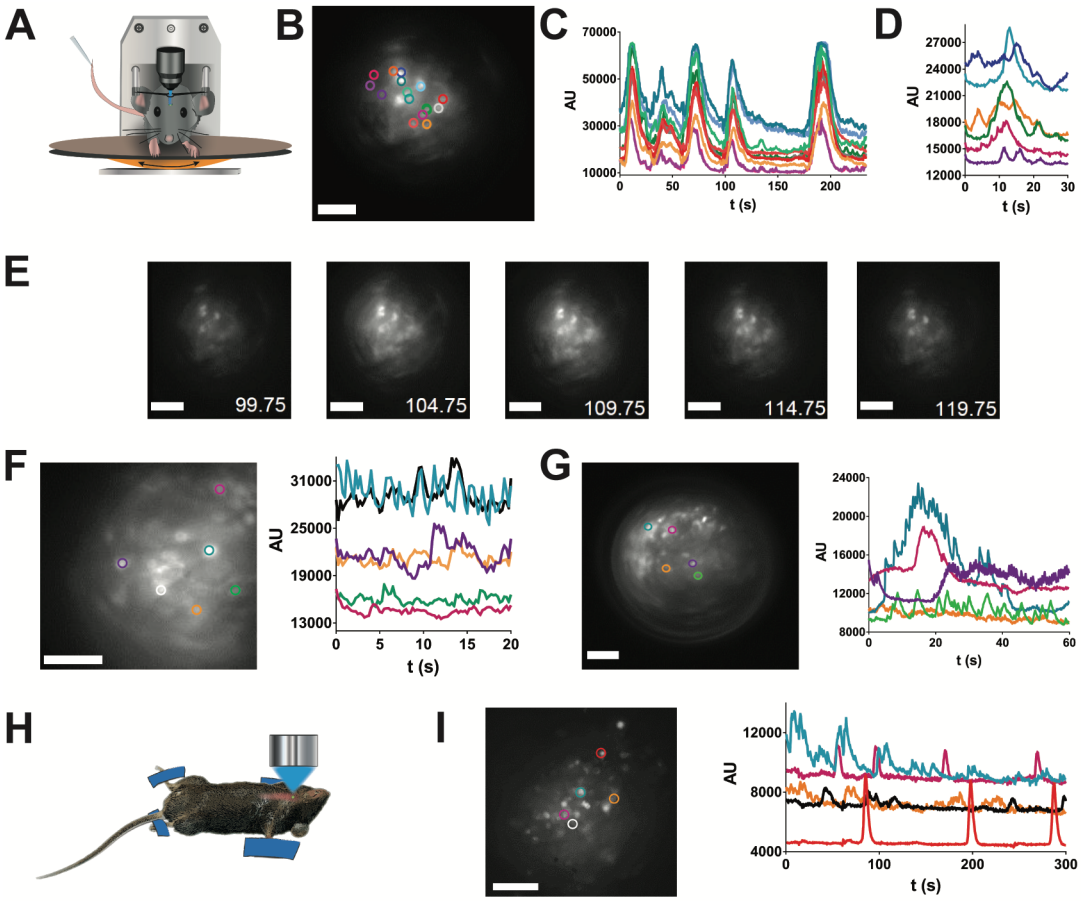
A
B
C
D
E
F
G
H
I
AU
t (s)
99.75
104.75
109.75
114.75
119.75

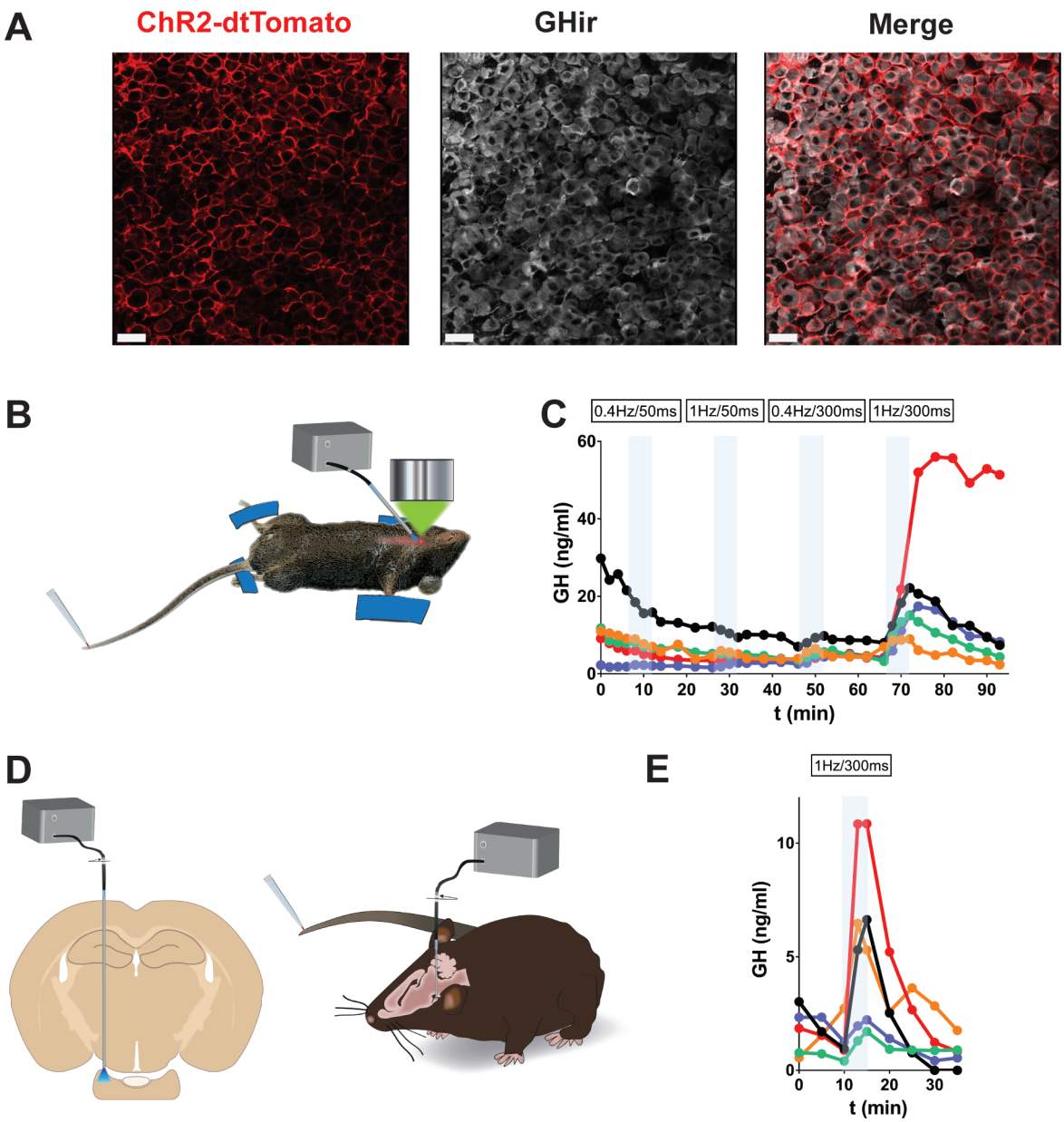
A
ChR2-dtTomato
GHir
Merge
B
C
0.4Hz/50ms
1Hz/50ms
0.4Hz/300ms
1Hz/300ms
GH (ng/ml)
t (min)
D
E
1Hz/300ms
GH (ng/ml)
t (min)

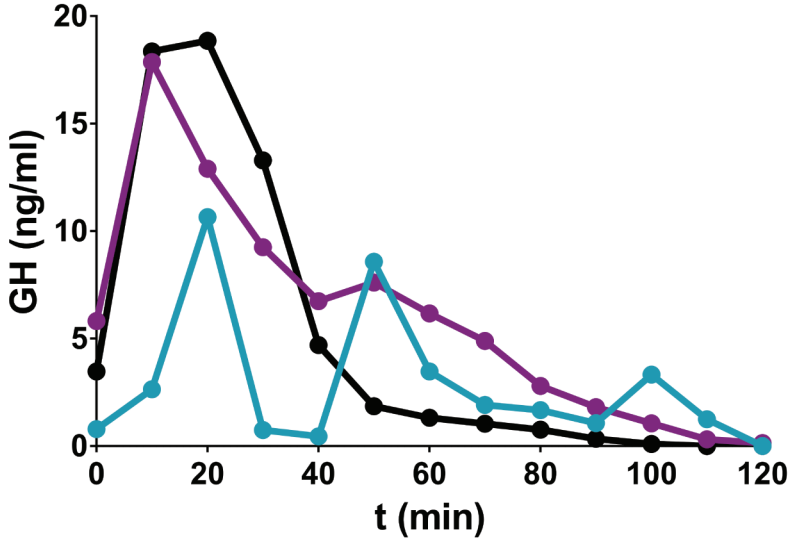
GH (ng/ml)
20
15
10
5
0
0
20
40
60
80
100
120
t (min)

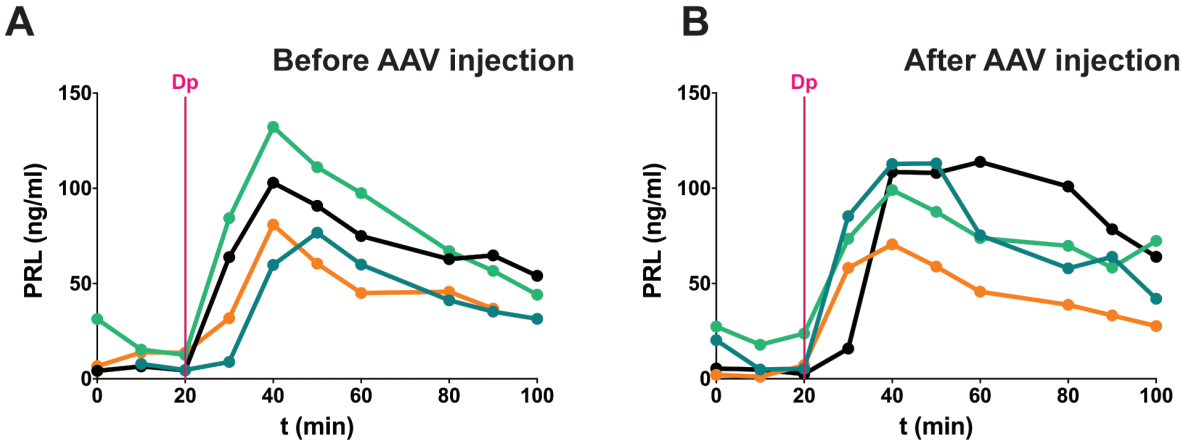
A
Before AAV injection
Dp
PRL (ng/ml)
150
100
50
0
0
20
40
60
80
100
t (min)
B
After AAV injection
Dp
PRL (ng/ml)
150
100
50
0
0
20
40
60
80
100
t (min)

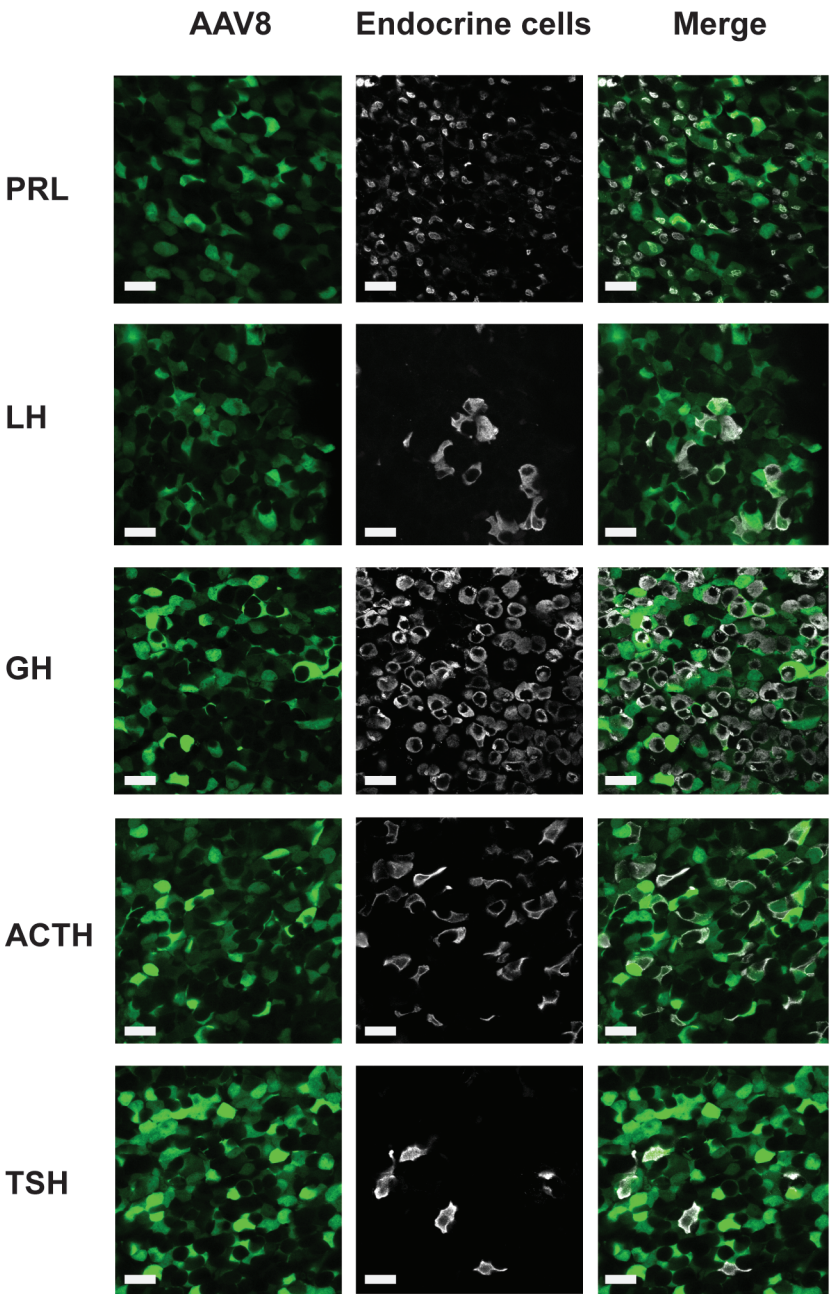
AAV8
Endocrine cells
Merge
PRL
LH
GH
ACTH
TSH

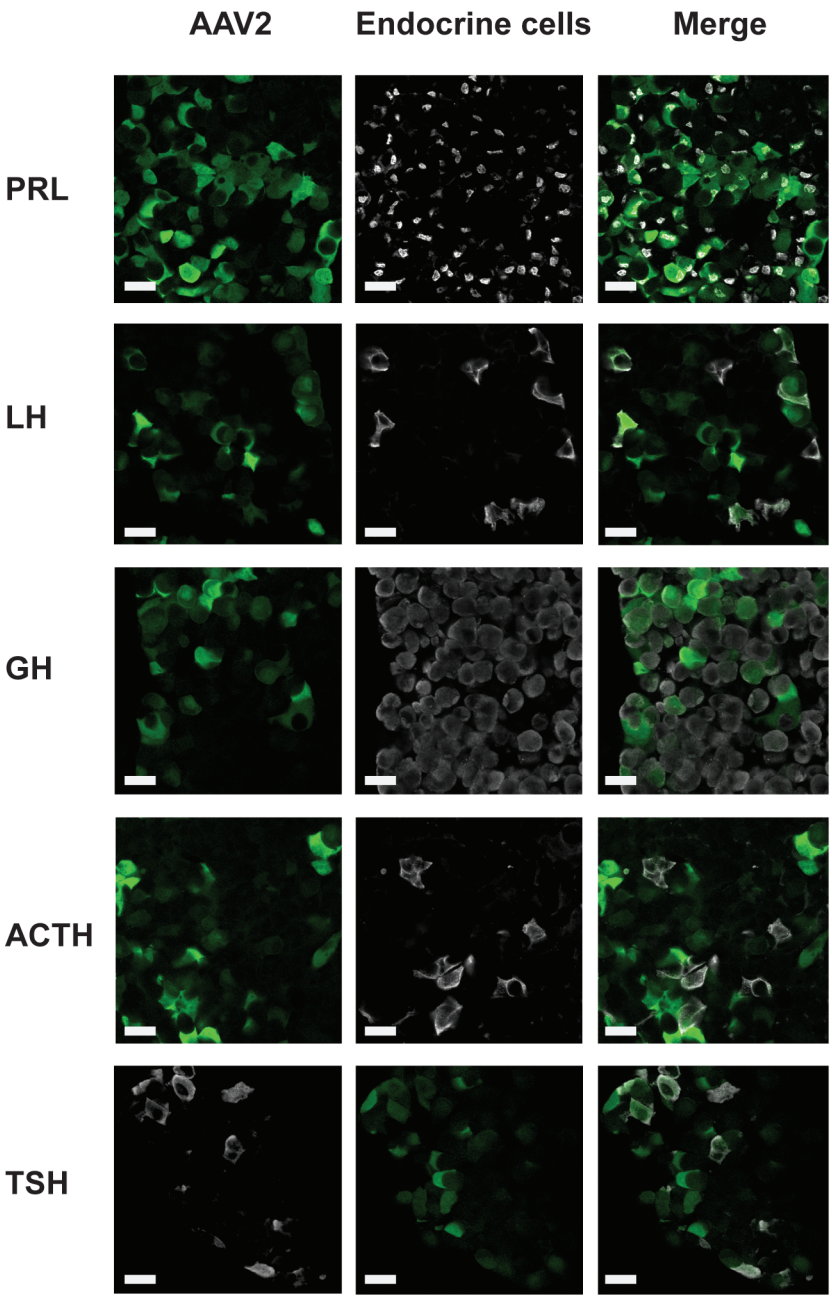
AAV2
Endocrine cells
Merge
PRL
LH
GH
ACTH
TSH

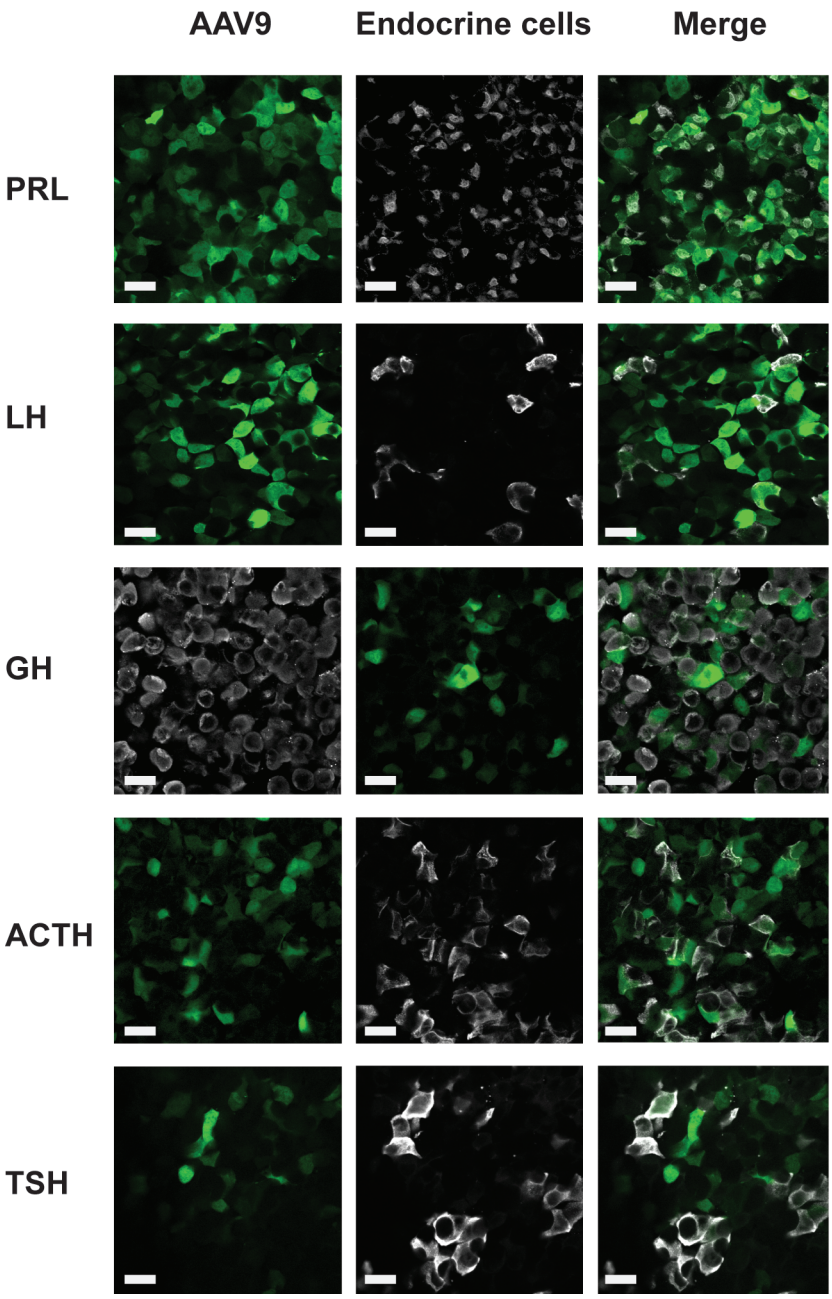
AAV9
Endocrine cells
Merge
PRL
LH
GH
ACTH
TSH

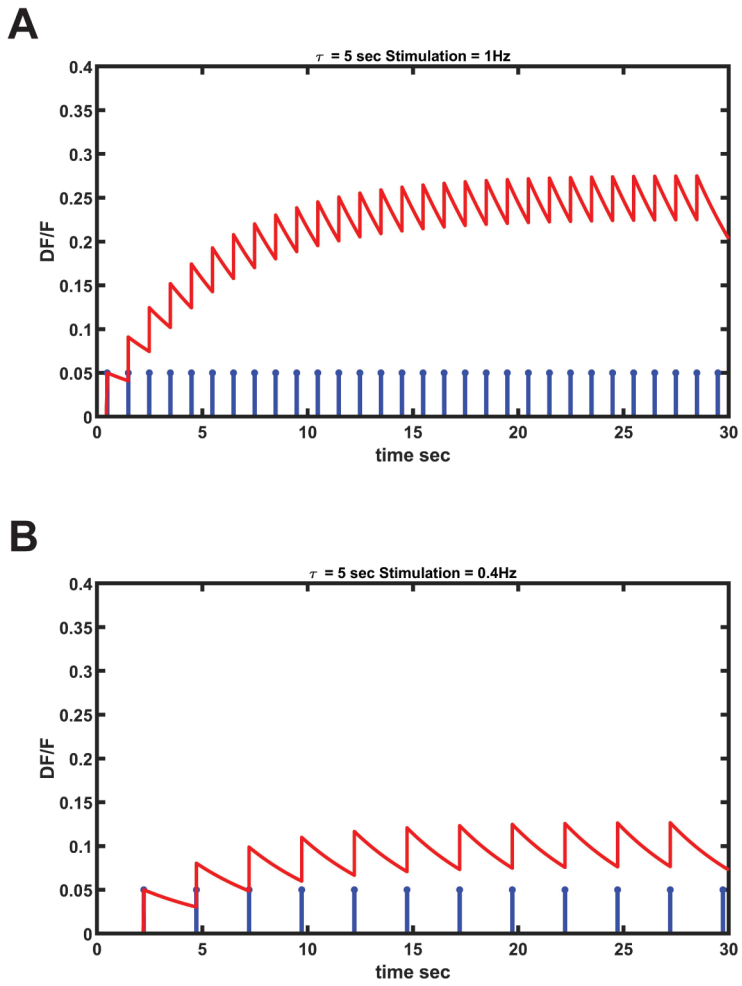
A
τ = 5 sec Stimulation = 1Hz
DF/F
time sec
B
τ = 5 sec Stimulation = 0.4Hz
DF/F
time sec